Influence of drug/lipid interaction on the entrapment efficiency of isoniazid in liposomes for antitubercular therapy: a multi-faced investigation.

Francesca Sciolla

CNR-ISC Sede Sapienza, Piazzale A. Moro 2, I-00185 - Rome (Italy)

Domenico Truzzolillo [1,*], Edouard Chauveau

Laboratoire Charles Coulomb (L2C), University of Montpellier, CNRS, Montpellier, (France)

Silvia Trabalzini

Dipartimento di Chimica e Tecnologie farmaceutiche, Università di Roma, Piazzale A. Moro 5, I-00185 - Rome (Italy)

Luisa Di Marzio

Dipartimento di Farmacia, Università G.d'Annunzio, Via dei Vestini, 66100 - Chieti, (Italy)

Maria Carafa, Carlotta Marianecci

Dipartimento di Chimica e Tecnologie farmaceutiche La Sapienza Università di Roma, Piazzale A. Moro 2, I-00185 - Rome (Italy)

Angelo Sarra

Istituto dei Sistemi Complessi (ISC), Sede Sapienza, CNR, Piazzale A. Moro 5, I-00185 - Rome (Italy)

Federico Bordi

Dipartimento di Fisica, La Sapienza Università di Roma, Piazzale A. Moro 2, I-00185 - Rome (Italy)

Istituto dei Sistemi Complessi (ISC), Sede Sapienza, CNR, Piazzale A. Moro 5, I-00185 - Rome (Italy)

Simona Sennato [2,*]

Istituto dei Sistemi Complessi (ISC), Sede Sapienza, CNR, Piazzale A. Moro 5, I-00185 - Rome (Italy)

Abstract

Isoniazid (INH) is one of the primary drugs used in tuberculosis treatment and its encapsulation in liposomal vesicles can both improve its therapeutic index and minimize toxicity. Here we consider mixtures of hydrogenated soy phosphatidylcholine/phosphatidylglycerol (HSPC/DPPG) to get novel biocompatible liposomes for isoniazid delivery. We determined INH encapsulation efficiency by coupling for the first time UV and Laser Transmission Spectroscopy and we showed that HSPC-DPPG liposomes can load more INH than expected from simple geometrical arguments, thus suggesting the presence of drug-lipid association. To focus on this aspect, which has never been explored in liposomal formulations, we employed several complementary techniques, such as dynamic and static light scattering, calorimetry and surface pressure measurements on lipid monolayers. We find that INH-lipid interaction increases the entrapment capability of liposomes due to isoniazid adsorption. Moreover, the preferential INH-HSPC dipole-dipole interaction promotes the modification of lipid ordering, favoring the formation of HSPC-richer domains in excess of DPPG. Our findings highlight how investigating the fundamental aspects of drug-lipid interactions is of paramount importance for the optimal design of liposomal nanocarriers.

Keywords: unilamellar liposomes, isoniazid, drug-lipid interaction, laser transmission spectroscopy, calorimetry, scattering techniques

*Corresponding author

[1]Laboratoire Charles Coulomb - UMR 5221, Universitè de Montpellier et CNRS, Place E. Bataillon, Campus Triolet, Batiment 11, cc 0026 34095 Montpellier Cedex 05, (France)
domenico.truzzolillo@umontpellier.fr

[2]Istituto dei Sistemi Complessi (ISC), Sede Sapienza, CNR, Piazzale A.

1. Introduction

Tuberculosis (TB) is caused by Mycobacterium tuberculosis, a bacterium often affecting the lungs. The World Health Organization estimates that about one-quarter of the world's population has active or latent TB, that caused the death of around 1.5 million people in 2019 [1]. The current TB-treatment is usually associated with serious adverse effects, resulting in poor compliance, onset of multidrug resistant strains and treatment failure [2]. Encapsulation of anti-TB drug in nanocarriers might be the modern answer for the development of innovative anti-TB strategies. Nanocarriers can improve the efficacy of the current TB treatments since they can be functionalized to bind mycobacterium-infected phagocites via biological ligands, and used for inhalation administration, or to enhance drug loading and pharmacokinetics, increasing significantly intracellular drug concentration. Since earlier studies proving a macrophage-specific delivery of anti-TB drugs [3, 4], liposomal vesicles still remain the most studied anti-TB nanocarrier. Moreover, the possibility to nebulize liposomal dispersions directly into the lungs offers a powerful route to overcome the several limitations of oral and intravenous administration of anti-TB drugs [5].

Isoniazid (INH) is one of the primary drugs used in the TB treatment and is well-known for its value in preventive therapy [6]. Being a small hydrophilic molecule with a low partition coefficient [7], INH is generally loaded in liposomes by the film hydration method [8]. In general, it is difficult to predict the amount of entrapped drug, since it may depend on the preparation method, the physico-chemical properties of the carrier (such as lipid composition, geometry and size) and the ionic force and pH of the dispersing medium. Actually, for any solvophilic drug, including hydrophilic ones, due to the small volume ratio between the internal volume of liposomes and that of the external medium, only a small amount of the drug is encapsulated.

Lipid composition has been recognized to be an important factor regulating drug loading and liposomes accumulation in the lungs [9]. It has been shown that administration of subtherapeutic INH doses entrapped in stealth liposomes composed by a mixture of phosphatidylcoline-pegylated distearoylphosphatidylethanolamine-cholesterol (PC-DSPE-PEG-Chol) and the anionic dicetilphosphate (DCP), is more effective than higher concentrations of the free drug [3, 10]. Later, several liposomal formulations based on DPPC, DSPC, EggPC, crude soy lecithin [11, 12, 13, 14], PE and DSPE-PEG [15] have been used to load INH efficiently. A rigorous comparison of the above results is difficult, especially for what concerns the entrapment efficiency, since they consider both multilamellar and unilamellar liposomes. However, it is evident that multilamellar vesicles ensure high drug entrapment due to the large volume of their aqueous compartments [13].

A further boost to the use of multilamellar vesicles has been given by both the possibility to co-encapsulate two anti-TB drugs as rifampicin and INH [12, 16], and the effective transport to the alveolar region of particles with diameters ranging from 0.1 to 2 μm through inhalation [5]. However, despite the advantages offered by multilamellar structures, these are far from being ideal carriers, since their size and the number of compartments cannot be controlled at will, raising precise regulatory issues [17]. For this reason, the development of optimal unilamellar liposomal vectors, able to entrap hydrophilic drugs, is highly desirable and still represents an important goal.

Beyond that, it was argued that the presence of a charged lipid could have a significant impact on the entrapment efficiency. Wasserman and coworkers [18] showed that the addition of a low content of anionic Cardiolipin in PC:Chol multilamellar liposomes yields a more efficient INH loading, since negatively charged bilayers produce wider aqueous spaces between lamellae, so to increase the volume of the aqueous compartments available for INH entrapment. Also, in anionic DPPG-HSPC multilamellar liposomes, a small amount of DPPG confers stability to the vesicles, without interfering with drug encapsulation during nebulization [19].

In this work we focus on mixed unilamellar HSPC/DPPG vesicles, which have not been explored as potential INH carrier so far. This formulation offers, at least, two advantages: i) HSPC is already employed in several approved liposomal drugs [20] and ii) the addition of DPPG gives allows exploiting polymeric chitosan coatings to confer mucoadhesion properties, which is relevant for pulmonary delivery [21].

In spite of the many different investigations on the preparation and the characterization of liposomal systems for *in vitro* and *in vivo* liposomal INH delivery, some crucial aspects concerning the physical-chemical properties of the carrier are still scarcely explored. To the best of our knowledge, an inadequate attention has been paid until now to understand the interaction of INH with the lipid bilayer of the carrier. Only few biophysical investigations report on the interaction of INH with liposomes mimicking a biological membrane, having the purpose to understand how the drug finds its way into a real membrane [22, 23, 24].

Our work leverages on an extensive characterization of the interaction between INH and HSPC-DPPG liposomes designed to optimize a novel INH delivery carrier for anti-TB therapy. After a preliminary characterization of liposomes by dynamic light scattering, UV and laser transmission spectroscopy, suggesting the presence of drug-lipid association, we focused on the interaction of INH with the lipid bilayers by taking advantages of differential scanning calorimetry, static light scattering and surface pressure measurements on Langmuir monolayers, through which we could unambiguously unveil the effect of INH on the thermodynamics of the mixed lipid membranes.

2. Materials and methods

2.1. Materials

Hydrogenated phosphatidylcholine from soybean (HSPC) and dipalmitoyl-sn-glycero-phosphorylglycerol sodium salt (DPPG) were a kind gift from LIPOID (details in SI). INH (pyridine-4-carbohydrazid, hereinafter INH, nominal purity 99%), Hepes

Moro 5, I-00185 - Rome (Italy), +39 06 49913503,
simona.sennato@roma1.infn.it

(N-2- hydroxyethyl, piperazine-N-(2-ethanesulphonic acid) and other chemicals were purchased by Sigma Aldrich and used without further purification.

2.2. Preparation of liposomes

Lipids were dissolved in chloroform/methanol/water (2/1/0.15 v/v/v) at varying DPPG molar fraction. Solvent was evaporated under vacuum and 60 °C, above the main transition temperature of lipids, to form a dried lipid film, which was rehydrated in 0.01 M Hepes, pH=7.4. To obtain unilamellar vesicles, the hydrated lipid suspension was homogenized by 5 cycles of freeze-thaw and extruded 10 times under nitrogen pressure through a 100 nm polycarbonate membrane (Whatman Nucleopore) in a 2.5 mL extruder (Lipex Biomembranes, Canada) at 60 °C, a process that does not produce appreciable changes in the initial lipid concentration [25]. To entrap INH, drug was dissolved in 0.01 M Hepes at pH=7.4 and then rehydration and extrusion followed as for empty liposomes.

2.3. Dynamic light scattering and electrophoretic mobility measurements

The hydrodynamic size and the ζ-potential of liposomal formulations were determined by dynamic light scattering (DLS) and electrophoretic measurements performed by a NanoZeta-Sizer apparatus (Malvern Instrument, UK) employing a a back-scatter detection. Hydrodynamic radius (R_h) and polidispersity index (PDI) are obtained by cumulant method [26]. ζ-potential is calculated by PALS analysis, as described in [27]. Results represent the average of three different measurements.

2.4. Laser transmission spectroscopy

The size and the absolute number concentration of liposomal suspension were determined using an innovative apparatus implementing the laser transmission spectroscopy (LTS) technique [28, 29]. Light transmittance through the suspension was measured by using a pulsed laser tunable in the wavelength interval from 210 to 2600 nm. Transmission data were analyzed and inverted by using a mean square root-based algorithm which gives the particle density distribution as a function of their size R through the Beer-Lambert law and the known Mie scattering cross section of the vesicles, modelled as shelled spheres [28]. The integral of the density distribution provided the total number of liposomes per milliliter of solution N_{LTS} [29, 30]. The volume fraction Φ_{in} of the liposomal dispersion available for encapsulation was calculated as $\Phi_{in} = N_{LTS} \cdot 4/3\pi(R-d)^3$, where d is the bilayer thickness.

2.5. Fluorescence anisotropy

Fluidity of liposomal bilayers has been evaluated by using diphenylhexatriene (DPH) probe located in the hydrophobic region of the lipid bilayer. 250 μL of DPH (2 mM) was added to lipid mixtures before vesicle preparation and DPH-loaded vesicles were prepared. A LS55 spectrofluorimeter (PerkinElmer, USA) was used to measure the fluorescence anisotropy (A) at 25 ^{o}C, defined as

$$A = \frac{I_{vv} - GI_{vh}}{I_{vv} + 2G}, \tag{1}$$

where I_{vv} and I_{vh} are the intensities of the emitted fluorescence parallel and perpendicular to the direction of the vertically polarized excitation light, respectively, and $G = I_{vh}/I_{hh}$ is a correction factor. The fluorescence anisotropy values are inversely proportional to the membrane fluidity and high values correspond to a high structural order and/or a large viscosity of the membrane [31].

2.6. Entrapment efficiency

Quantification of INH loaded in liposomal formulations was carried out by a UV-VIS Jasco spectrophotometer with 1 mm quartz cuvettes, at 20 °C. To subtract the background scattering contribution, we measured spectra of empty liposomes measured in a wide concentration range (1 to 20 mg/ml), with Hepes buffer as reference. Drug concentrations before and after purification have been determined by considering the INH absorption peak at $\lambda \sim 264$ nm [32].

Entrapment efficiency (E.E.) has been calculated as

$$E.E.(\%) = \frac{C^f_{INH}/C^f_{lipid}}{C^0_{INH}/C^0_{lipid}} \cdot 100, \tag{2}$$

where C^0_{INH}, C^0_{lipid} and C^f_{INH}, C^f_{lipid} refer to the molar concentration of INH or lipid, before and after purification, respectively.

2.7. Differential scanning calorimetry

Differential scanning calorimetry (DSC) measurements were carried out by a TA Q2000 calorimeter by performing 3 heating/cooling cycles under nitrogen flux by a modulated temperature protocol (amplitude= 0.3 °C, rate = 2 °C/min), over a 60 s period in the temperature range 10-70 °C. Excess molar calorimetric enthalpy was calculated after baseline adjustment and normalization to the lipid concentration by integrating the peak areas. The transition temperatures (T_m) were determined at the peak maxima of the heat capacity curves.

To investigate the drug-lipid interaction, we added 10 μl of INH at varying concentration to 500 μl of unilamellar liposome suspension at 10 mg/mL.

2.8. Static light scattering

Static light scattering (SLS) experiments have been performed using an Amtec-goniometer (laser wavelength $\lambda = 532.5$ nm) and a thermostatted cell. We fixed the incident light intensity and collected the time-averaged scattering intensity $I(q)$ by dilute unilamellar liposomes samples (0.2 mg/ml) at 60 scattering angles between 24° and 150°, being q the scattering vector. R_g was determined by the Guinier approximation $I(q) = I(0)\exp[-(qR_g)^2/3]$ [33]. As for DSC, a proper INH amount was added to liposomes to investigate the effect of the drug.

2.9. Monolayer studies

We performed surface pressure measurements by a Mini-trough (KSV Instruments, Finland) equipped with Wilhelmy plate and thermostatted at 25.0 ± 0.2 °C. Mixed HSPC-DPPG lipid monolayers were prepared by Langmuir technique [34] as

previously described [35]. 20 μl of lipid dissolved in chloroform at 1 mg/ml was spread on the Hepes subphase and the monolayers were compressed at 50 mm min^{-1} to record the pressure/area (Π/A) isotherm, after solvent evaporation.

To study INH interaction with monolayer, we dissolved INH in ethanol at its maximum solubility concentration ($\sim$ 67 mM) and injected a proper volume in the subphase under the lipid film. Ethanol is less dense than water and highly volatile, thus favoring INH spreading. Control experiments by injecting different volumes of pure ethanol have been performed to quantify the extent of pressure increase.

To get information on lipid miscibility, we calculated the excess of mixing free energy ΔG upon integration of the Π-A isotherms from zero to $\pi = 35mN/m$, i.e the pressure correspondent to the packing density of lipid bilayers [36]. This reads

$$\Delta G = \int_0^{35} (A_{12} - X_1 A_1 - X_2 A_2) d\pi, \quad (3)$$

where A_i and X_i are the area per molecule and the molar fraction of component i, respectively, and A_{12} is the area per molecule in the mixture. In the absence of any interaction between the lipid components $\Delta G = 0$, while deviations from an ideal behavior result in $\Delta G < 0$ (attractive interactions) or in $\Delta G > 0$ (repulsive interactions), providing information on whether mixing is energetically favored or not [37].

3. Results

3.1. Basic characterization of HSPC-DPPG liposomes

Size, polydispersity, ζ-potential and fluorescence anisotropy of empty unilamellar liposomes have been measured for three different X_{PG} molar fractions at T=25 °C (Table 1). We obtain unilamellar liposomes with size around 100 nm and a low polydispersity index, as confirmed by TEM microscopy (SI-2).

X_{PG}	$R_h(nm)$	PDI	ζ-pot (mV)	Anisotropy	E.E. (%)
0.33	57 ± 3	0.08 ± 0.01	-35 ± 4	0.37 ± 0.04	2.4 ± 0.2
0.50	55 ± 2	0.07 ± 0.01	-53 ± 6	0.35 ± 0.05	1.7 ± 0.2
0.66	52 ± 2	0.11 ± 0.02	-42 ± 4	0.37 ± 0.03	1.1 ± 0.1

Table 1: Characterization of empty HSPC-DPPG liposomes and E.E. values for liposomes prepared at ρ=10 (200 mM INH). Results represent the mean values over three repeated measurements. No significant variation has been observed on size and ζ-pot values of INH-loaded liposomes (data not shown).

The values of ζ-potential are negative for all the three formulations, due to the presence of the anionic lipid DPPG. The higher ζ-potential value observed at the equimolar formulation is indeed not very surprising. We have already shown [35] that while the stoichiometric charge increases linearly with the charged lipid content, the effective charge of liposomes displays a saturation due to the counterion condensation which tends to minimize the repulsion between the nearby negative charges on the membrane. At the same time, the membrane ζ-potential is affected by the dipolar orientation of the zwitterionic head groups that are susceptible to any variation of the local composition within the membrane [38, 39]. Thus, in general the measured ζ-potential is not necessarily affine to the amount of ionic headgroups in the bilayer. This said, such an aspect deserves surely a deeper investigation that does not represent the focus of this work

The observed high values of anisotropy point out that all the formulations have a rather rigid lipid bilayer, as the pure components DPPG, DPSC and DPPC liposomes [40]. This is indeed expected since both lipids are in a gel state at 25 °C. The slightly higher values observed at the equimolar composition may be connected to the maximum degree of disorder that it is expected in this condition, that will be clarified by DSC analysis.

We performed a preliminary set of experiments to determine the best condition for encapsulation of INH within the range $1 \div 50$ of INH/lipid molar ratio ρ (SI-3). Table 1 reports the highest values of entrapment efficiency found at intermediate excess of drug, at ρ=10. In general, we found low $E.E.$ values. The highest value of $E.E.$ is found at the lowest content of the charged lipid DPPG and a decreasing trend with increasing X_{PG} is observed. This could indicate a worse retention capability of the vesicles due to the looser packing in more charged bilayers. In fact, electrostatic repulsions between charged lipids alter the bilayer properties and may increase permeability to solutes [41]. However, this hypothesis does not appear suitable since the anisotropy values of HSPC-DPPG liposomes close to 0.36 indicate a rather rigid bilayer. Moreover, it has been shown that INH does not induce any change in fluidity in DMPC and DMPG liposomes [22], which are more fluid and with lower melting temperature compared to HSPC and DPPG lipids.

From an operative point of view, E.E. parameter values are useful to select a mixture to get the highest amount of entrapped INH, given a fixed mass of lipid and drug employed in the sample preparation. Such an optimal mixture is reached for X_{PG}=0.33. On the other hand, the only determination of E.E. does not allow unveiling how the amount of entrapped drug is influenced by the physico-chemical properties of the lipid bilayer, namely the size, total volume and the lipid composition of the carriers.

3.2. LTS study of INH-loaded liposomes

To get further insight on the encapsulation properties of HSPC-DPPG liposomes, we performed LTS experiments on INH-loaded liposomal suspensions prepared at ρ=10, where the highest values of drug entrapment is reached regardless of lipid composition. The aim of this study is to determine the radius R and the total number of liposomes per milliliter of solution N_{LTS}, and then calculate the liposome volume fraction available for encapsulation Φ_{in}, as detailed in section 2.4. Once the volume fraction is obtained, it is possible to define a parameter named 'Entrapment ratio' (hereinafter E.R.) as the ratio between the concentration of drug encapsulated in the vesicles (determined by UV) and the maximum amount of drug which

X_{PG}	R (nm)	$N_{LTS}\,(part/ml)$	$INH/Lip\,(mM/part)$	Φ_{in}	E.R.
0.33	45 ± 4	$(2.7 \pm 0.2)\,10^{12}$	$(1.8 \pm 0.2)\,10^{-16}$	$(0.73 \pm 0.07)\,10^{-3}$	3.3 ± 0.3
0.50	40 ± 4	$(1.0 \pm 0.1)\,10^{13}$	$(1.4 \pm 0.2)\,10^{-16}$	$(1.8 \pm 0.2)\,10^{-3}$	3.8 ± 0.4
0.66	37 ± 3	$(6.6 \pm 0.6)\,10^{12}$	$(0.9 \pm 0.1)\,10^{-16}$	$(0.91 \pm 0.09)\,10^{-3}$	3.3 ± 0.3

Table 2: Results of LTS study of INH-loaded liposomes prepared at $\rho = 10$ (200 mM INH): radius of liposomes R; total number of liposomes per milliliter N_{LTS}; INH liposomal amount INH/Lip; liposome volume fraction Φ_{in}; entrapment ratio $E.R.$

can be loaded in their internal volume

$$E.R. = \frac{C^f_{INH}}{C^0_{INH} \cdot \Phi_{in}} = \frac{E.E.\%}{100 \cdot \Phi_{in}}. \quad (4)$$

By this definition, E.R. can give indications on the entrapment efficacy of a lipid membrane with a specific lipid composition, independently of its geometrical features. We will show that the E.R. is of valuable help for our analysis.

Table 2 shows values of $E.R.$ calculated by assuming a bilayer thickness d of 5 nm, corresponding to the average value reported for pure DSPC and DPPG bilayers [42]. The radius of liposomes determined by LTS has a behavior similar to the hydrodynamic radius measured by DLS (table 1), though it is shifted to smaller values, as expected since LTS gives the distribution of the geometrical sizes of the suspended particles and not the radius of a full sphere with the same diffusion coefficient as liposomes [30].

Thanks to the determination of the liposome concentration (N_{LTS}), we can do a step further and calculate the 'INH liposomal amount' (INH/Lip), i.e. the amount of INH loaded in each liposome, by dividing the total concentration of INH determined by UV measurements with respect to N_{LTS}. We note that the values of INH/Lip decrease with increasing X_{PG}, this could be due to the geometrical radius which decreases, too. At the single-nanocarrier level, we must conclude that liposomes with the lowest content of the charged lipid can retain more INH.

In order to filter out the effect of the geometrical features of liposomes, namely their volume and number, we can perform a further analysis of the drug encapsulation by considering the E.R. parameter. First, it is noteworthy that $E.R.$ is always higher than unity, that is the value corresponding to the absence of drug-lipid interaction and drug leakage [42]. Secondly, we note that the E.R. values are similar and comprised between 3 ad 4. Considering that in the pre-purified liposomal dispersion INH is added in large excess, the high E.R. values mean that vesicles can retain around and/or within lipid bilayers about three times more molecules than the amount of drug expected on the basis of the geometrical volume thus pointing out the preferential interfacial localization of INH. Finally we note that for the equimolar mixture E.R. is slightly higher than for asymmetrical formulations.

Since the E.R. analysis allows comparing different liposomal suspensions as if they were composed by the same number of identical vesicles and it is built to unveil the influence of bilayer properties in drug entrapment, our results show that liposomal vesicles at equimolar HSPC-DPPG ratio are the most effective for INH entrapment.

To sum up, our findings indicate the presence of drug-lipid attractive interactions and suggest that INH adsorb at the liposome interface [42]. As argued by Truzzi et al. [16] in PC-Chol multilamellar vesicles, drug-lipid affinity could originate drug adsorption. Hereafter we will show that this is indeed what occurs here, corroborating this finding by an extensive study of the organization of lipid layers and their interaction with INH.

4. Investigation of the effect of INH-lipid interaction

4.1. Differential scanning calorimetry

To understand the fine details of the local structure in the absence of INH, multilamellar HSPC-DPPG liposomes have been considered to get the highest DSC signal. However, no detectable difference has been observed with respect to the behavior of unilamellar liposomes which represent a more reliable modelling of the conditions characterizing the carriers (SI-4). Fig. 1 shows the excess molar heat capacity C_p of multilamellar liposomes at different X_{PG}.

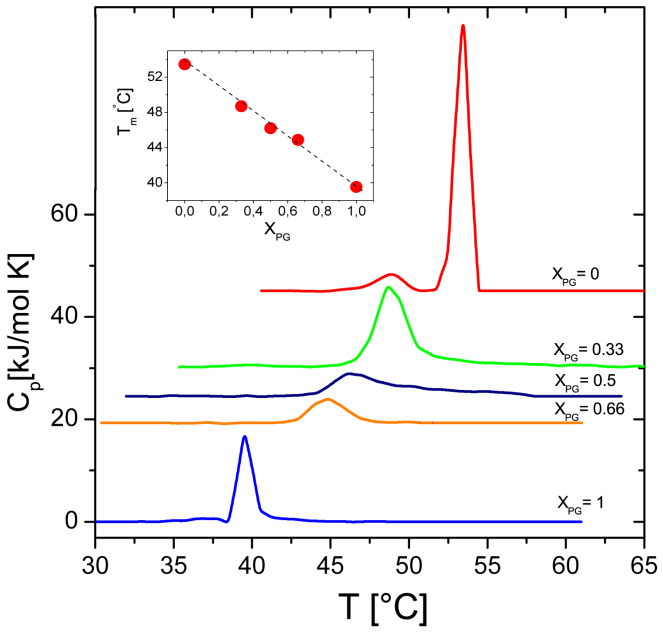

Figure 1: Excess molar heat capacity (main panel) and melting temperatures (inset) of pure and mixed multilamellar liposomes (lipid concentration= 25 mg/ml). Curves are shifted by a constant value.

HSPC liposomes exhibit two endothermic peaks corresponding to the pre- and main transition at 48.8 °C and 53.4 °C, respectively. The endothermic peak progressively shifts to lower

temperatures with increasing X_{PG}, it broadens down to X_{PG} = 0.50 and sharpens again as the system approached pure DPPG membranes ($X_{PG} \geq 0.33$). At the same time the pre-transition observed for pure HSPC multilamellar liposomes [43] vanishes as the fraction of DPPG is raised. The main endothermic transition never shows peak splitting or two detectable separate peaks, while linearly shifts to lower transition temperatures for increasing X_{PG} (inset Fig. 1). This feature supports the full miscibility of the two lipids that melt cooperatively in the bilayers, and it is corroborated by the minimum of the peak height occurring at the equimolar condition, where the broadness of the process is maximum. This suggests that at equimolar condition lipid miscibility is the highest, and lipid disorder is maximum, too.

Fig. 2 shows the excess molar heat capacity for mixed liposomes at selected ρ. First we note that INH addition does not alter the shape and the position of the main transition peak, thus confirming liposome stability, but its effect on lipid miscibility is surprising. The thermograms do not undergo any noteworthy variation for the equimolar mixture, whereas at X_{PG} = 0.33 the main peak shows a right shoulder and at X_{PG} = 0.66 strikingly peak splitting occurs. The latter appears at any INH content and is a signature of lipid segregation induced by drug-lipid association.

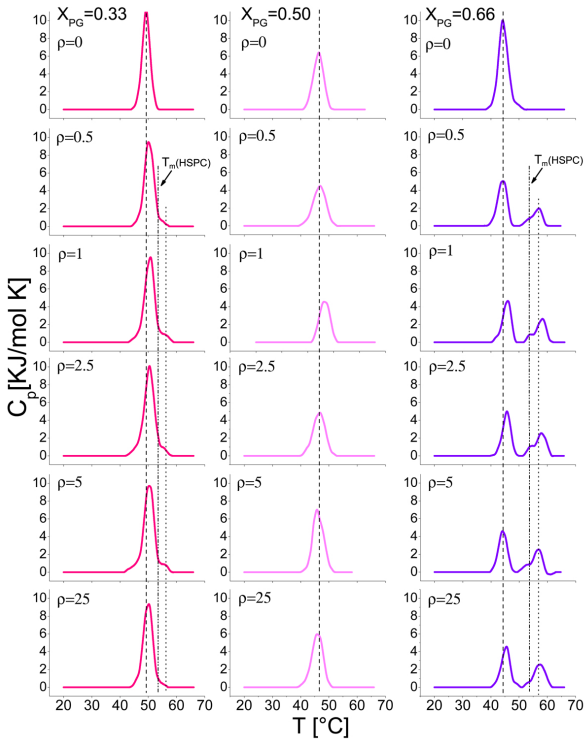

Figure 2: Excess molar heat capacity of unilamellar liposome suspensions (10 mg/ml) for different DPPG molar ratio X_{PG} and INH/lipid molar ratio ρ as indicated in the panels. As eyes guide, the position of T_m is identified by vertical lines: main peaks at ρ = 0: dash; T_m of pure HSPC liposomes: dash-dot; secondary peak appearing at $\rho \geq 0.5$: dot.)

To interpret this complex behavior, one has to consider that the chosen protocol provides that INH is added to suspensions of previously formed unilamellar liposomes (as described in section 2.7), thus imposing that its interaction occurs preferentially with the external lipid layer, while the inner layer stays scarcely affected by INH. Moreover, since the mismatch between the alkyl chains is very small, the outer and the inner layer are weakly coupled and they can show different thermodynamic phases [44].

On the basis of the DSC thermograms, we can hypothesize the formation of super-bound INH-HSPC-rich phases in the outer lipid layer with a T_m higher than pure HSPC, as suggested by the secondary peaks appearing at $\rho \geq 0.5$ at X_{PG} = 0.66 (Fig. 2, dotted line). At X_{PG} = 0.33 the fraction of INH-HSPC-rich phases is low and the mixed HSPC-DPPG phase prevails, since a complete HSPC segregation would imply that charged DPPG molecules to get closer and closer, this configuration being unfavored due to the high energetic and entropic penalty. At X_{PG} = 0.66, the situation is even more complex since bare HSPC molecules segregate in a distinct phase, as evidenced by the left-shoulder of the secondary peak centered at the T_m of pure HSPC. For both asymmetrical mixtures the segregated phases coexist with mixed HSPC-richer and DPPG-richer phases, respectively, which are shifted to higher temperatures due to the INH screening, as the main DSC peaks indicate.

It is therefore evident that the presence of INH at liposome interface and its interaction with lipids play a key role. Previous investigations have suggested a superficial distribution of INH in pure zwitterionic DMPC or anionic DMPG liposomes [7] and hypothesized a lipid packing modification in DPPC liposomes due to interaction between the drug and the phosphate region of the lipid heads via van der Waals or hydrogen bonding [16, 45]. Although at physiologic pH INH is neutral [24], its charge distribution has been considered relevant for the interaction with drug receptors and lipid membranes [46]. In particular, INH has a larger dipole moment than water [47], originating from the deformation of the electronic charge distribution in the vicinity of the electronegative O(1) and N(1) atoms [46]. In the presence of HSPC-DPPG mixed bilayers and in aqueous environments, it is then reasonable to consider that a dipole-dipole interaction between INH molecules with the zwitterionic HSPC lipids is favored, as already observed for other dipolar molecules such as anesthetics [48]. We speculate that this preferential attraction can promote the formation of quadrupolar INH-HSPC complexes and increases the binding energy between HSPC lipids, thus favoring the segregation of the HSPC at molar excess of DPPG, as the secondary peak at $T > T_m^{HSPC}$ suggests. On the other hand, the positive region of INH dipole can interact also with the anionic polar head of DPPG, thus stabilizing the DPPG-richer phase by electrostatic screening. A simple naive scheme of this situation is sketched in Fig. 3.

Lipid segregation or enhanced disorder typically shift the melting transition temperature of the single lipids, which reflects the formation or disruption of homogeneous domains [49]. To understand this point, we defined ΔT_m as the difference $T_m^{\rho} - T_m^{\rho=0}$ between the melting temperature of lipid membranes in presence of INH and for ρ = 0 (no added INH). Fig. 4 shows that INH addition produces a positive shift of the melting temperature for asymmetric mixtures. This suggests that primar-

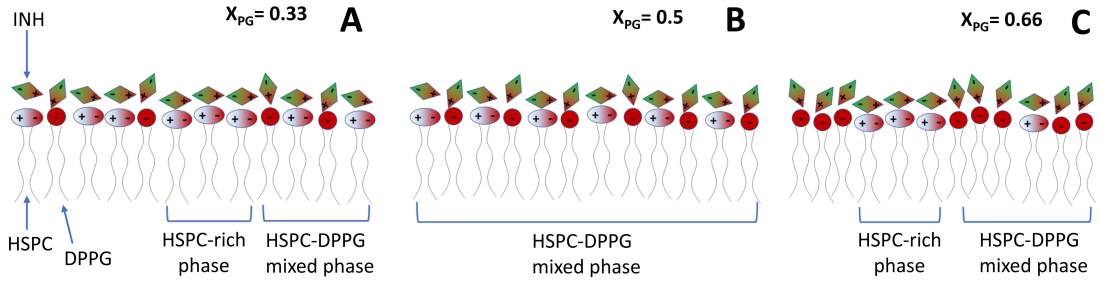

Figure 3: Schematic picture modelling the effect of INH addition on lipid organization.

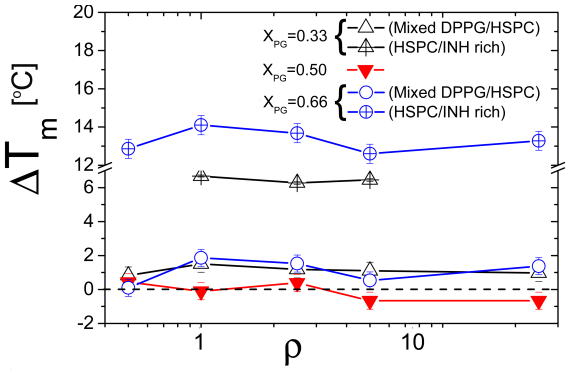

Figure 4: Melting temperature shift in function of the INH/lipid molar ratio ρ at different X_{PG}.

ily INH screens electrostatic repulsions between the phosphate groups decorating the membrane surfaces, lowering the effective surface charge of the liposomes and enhancing lipid local order [50]. As also observed by Pinheiro et al. [24] for DPPC liposomes, a $\Delta T_m > 0$ indicates the presence of drug at the lipid interface in the chain region (C1-C9) close to the polar heads.

The largest increase is obtained for the HSPC-rich domains appearing in the mixtures at $X_{PG} = 0.33$ and $X_{PG} = 0.66$, where lipid demixing takes place, while for X_{PG} =0.5 this shift is barely detectable or even weakly negative for large ρ values, suggesting that the high mixing entropy of the mixture in this case dominates over any enthalpic change due to the INH insertion [51]. Such a negative trend is presumably the signature of a local disorder induced by the INH insertion in the bilayer, that facilitates the melting transition.

Our findings thus indicate that unbalanced interactions between lipids and an external agent (INH here) are very important in determining the lipid local order within the membrane, as they typically favor segregation of one of the two species, as also reported for DNA-cationic liposome complexes [49, 51, 52, 53, 54]. Indeed, we may speculate that, similarly to nucleic acid-lipid mixtures [49, 51], INH molecules could affect more intimately the lipid bilayer structure than simply enhancing electrostatic screening by molecular insertion, favoring disorder and nucleation of defects and facilitating the transition to the melt state of the mixed and most heterogenous bilayers.

4.2. *Static light scattering*

We determined by SLS the liposome gyration radius R_g for each formulation both in the absence of INH and at $\rho = 5$ (Fig. 5). First we note that R_g is affected by the melting of the bilayers as evidenced by its sharp increase close to T_m (see SI for details). Secondly, INH addition always gives rise to an increase of R_g of the liposomes. This rules out i) the simple electrostatic screening effect due to the INH localization within a diffuse layer around the liposomes, since it would facilitate the lipid compactness within the bilayer and hence an overall decreases of the liposome size, and ii) an osmotic effect due to the excess of solutes outside the liposomes giving rise to the partial evacuation of water from the interior of the liposomes [55] and hence to their shrinkage. On the other hand, the increased size suggests that INH accumulates on liposome surface, possibly penetrating in the bilayer. In fact, both superficial adsorption and/or partial insertion of INH within the bilayer would give an increase of the liposome size. Once again, this result corroborates the scenario where INH strongly interacts with mixed HSPC-DPPG bilayers and affects their internal structure.

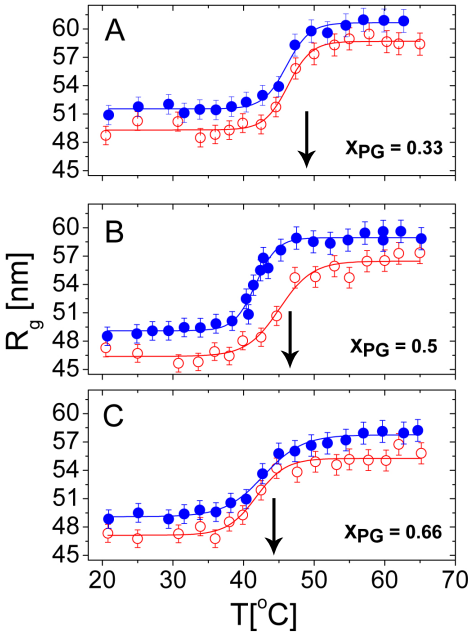

Figure 5: Gyration radii of mixed HSPC-DPPG unilamellar liposomes for $\rho = 0$ (◯) and $\rho = 5$ (•).

4.3. Monolayers

To further clarify the interaction of INH with both the lipids, we have studied isotherms of pure and mixed HSPC-DPPG monolayers at air-water interface in the presence of INH. We injected INH under the monolayers in the liquid-expanded phase to observe the maximum extent of drug-lipid interaction, since the low lipid density of the monolayer facilitates drug-lipid association [23]. Preliminarily, we have tuned the INH/lipid molar ratio ρ by injecting increasing volumes of INH (SI-5). Fig. 6 shows isotherms obtained after injecting the maximal amount used in monolayer experiments (200 μl of 0.013 mM INH), for mixed (panels A-B-C) and one-component monolayers (panels D-E). To evaluate the net effect of INH, isotherms obtained after the injection of the same volume of pure ethanol are shown for comparison. Ethanol is a surface-active compound and it may interact with the lipid monolayers [56]. It is evident that the injection of INH or ethanol causes a shift to larger areas per molecule, at a given surface pressure. This effect is commonly attributed to the adsorption of the injected molecule at the interface and is enhanced by the interaction between the drug and lipid layers, as also claimed by Chimote et al. [23] and by Marques et al. [45], who suggested an intercalation of INH close to the polar head of DMPC liposomes. Since here INH is in large excess with respect to the lipids, its insertion may occur, followed by a lipid realignment upon compression.

We observe that Π-A isotherms of pure DPPG and HSPC liposomes in the presence of INH are systematically shifted to larger areas with respect to those of bare liposomes. This indicates that the drug is located in some extent within the lipid layer. Moreover, if this effect is still present in the condensed phase, it evidences that drug molecules remain inserted during compression and occupy an additional space in film. In mixed monolayers this effect depends somehow on the DPPG content and is suppressed upon decreasing the DPPG fraction. However more generally we do not expect a large exchange of INH molecules between the interface and the bulk during compression since the duration of the latter is far shorter than the time waited to reach an equilibrated monolayer before any compression. For $X_{PG} = 0.33$, the isotherm recorded when INH is added converges towards that of the bare monolayer at high surface pressure. This could be attributed to a drug 'squeezing out' during compression or to a peculiar rearrangement between the drug and the lipids, which minimizes the overall molecular hindrance.

Fig. 6-F shows the excess free energy ΔG for HSPC-DPPG monolayers in the presence and the absence of INH and ethanol. HSPC-DPPG monolayers (○) on Hepes subphase show an almost ideal-behavior with ΔG approaching zero at low PG content and a slightly higher negative deviation for $X_{PG} = 0.66$, indicative of attractive interactions between the two lipids which can stabilize the mixed film. This confirms the results obtained by DSC indicating a full miscibility of the lipids (see section 4.1) and it is in agreement with simulations [57], showing that demixing does not occur when the compositional mismatch between the alkyl chains of membrane lipids is lower than 6 carbons.

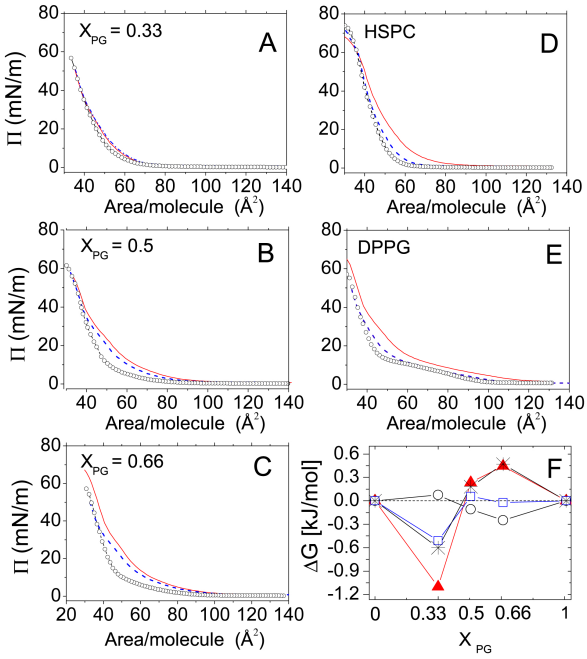

Figure 6: Surface pressure isotherms of mixed HSPC-DPPG monolayers (A-B-C) and pure lipids (D-E) on Hepes subphase (◯) and after injection of 200 μl of ethanolic INH or pure ethanol (full and dashed line, respectively). Isotherms represent the average over three experiments. Panel F shows the excess free energy of mixing ΔG calculated for HSPC-DPPG monolayers on Hepes ◯) and after injection of 200 μl of INH solution (▲) or ethanol (□). The difference $* = ▲ - □$ evaluates the INH effect.

The addition of a polar compound as ethanol and INH (□, ▲, respectively) causes deviations from the ideal behavior, indicating the onset of non-negligible interactions between the solutes added in the subphase and the lipid film. The large negative deviations at $X_{PG} = 0.33$ in the presence of INH indicate that HSPC-DPPG bonds are preferred with respect to HSPC-HSPC and DPPG-DPPG ones. This is not in contrast with the onset of super-bound INH-HSPC states observed in DSC thermograms for this lipid formulation, since in large excess of HSPC the presence of such states is statistically favored even without lipid demixing.

Conversely, beyond equimolarity, the positive deviations of ΔG indicate that interaction between lipids of the same kind are favored and may cause lipid segregation. The latter indeed can be induced when a positive ΔG is of the order of $K_B T$ at T=298 K, as in our system, in line with Monte Carlo simulations of binary lipid mixtures [58]. In agreement with DSC results, this finding indicates that INH-lipid interaction can modify the miscibility of HSPC and DPPG.

We have discussed in section 4.1 how attractive interactions between the dipoles of INH and HSPC can promote the formation of quadrupolar INH-HSPC complexes and increases the binding energy between HSPC lipids. However it's worth stressing that this mechanism can favor the segregation of a HSPC-rich phase in excess of DPPG, as indicated by the positive values of ΔG at $X_{PG} = 0.66$. While the condensation of the relatively few HSPC lipids 'diluted' in a enriched DPPG matrix is entropically and energetically costly in the absence of INH,

the formation of attractive complexes and screening of electrostatic repulsions between DPPG molecules is favored when INH is added. Conversely, in excess of HSPC, the addition of INH does not cause lipid demixing because the condensation of the DPPG molecules, now acting as repulsive 'defects', would always imply an high energetic and entropic penalty. In this condition, the negative value of ΔG suggests a stabilization of the mixed film by screening the electrostatic repulsions between DPPG molecules.

All in all, these findings corroborate the scenario in which the strong lipid demixing observed in unilamellar liposomes at $X_{PG} = 0.66$ and in the presence of INH, is driven by the modification of lipid-lipid interaction due to INH-HSPC binding.

5. Conclusion

We investigated the encapsulation of the antitubercular drug isoniazid (INH) in charged unilamellar vesicles composed by zwitterionic HSPC and anionic DPPG lipids, and its interaction with the lipid bilayers. For the first time the amount of drug encapsulated in the vesicles has been compared with the one expected from liposome volume fraction measured by LTS. We found that the encapsulation of INH is an unexpectedly efficient process, indicating that drug-lipid interaction is relevant.

INH accumulates at the lipid interface, affects its thermodynamics and can induce lipid segregation in excess of the anionic DPPG, in a complex interplay between electrostatic screening, entropy, lipid-lipid and drug-lipid interaction. Conversely, in excess of HSPC and at equimolar composition, screening effects prevail, with the two lipids remaining mixed. The results obtained on HSPC-DPPG monolayers corroborated such a scenario, with a phase separation favored in excess of DPPG, while the maximum heterogeneity of the lipid layer and a larger INH insertion in the bilayers at equimolar composition may explain the larger value of the entrapment ratio found for INH-loaded liposomes. The dipolar nature of INH at physiological pH [46, 59] favors a dipole-dipole interaction with zwitterionic lipids. We have proposed that the preferential INH-HSPC interaction induces the formation of ultrastable quadrupolar complexes, characterized by a high melting temperature.

At the best of our knowledge, our investigation represents the first piece of evidence on the effect of INH on the lipid organization in charged PC-based liposomes to be possibly employed as anti-TB nanocarriers. Our work points out the crucial importance to investigate drug-lipid interfaces to improve the design of a nanocarrier, and to achieve an in-depth understanding of drug-bilayer interactions to develop more efficient drugs and drug delivery systems. The ability to understand the modifications induced by drug/lipid interaction could help in finding strategies to modulate bilayer stability and permeability, and to stabilize the liposome bilayer during circulation [60, 61].

CRediT authorship contribution statement

F. Sciolla, E. Chauveau, S. Trabalzini, A. Sarra: investigation, data analysis; D. Truzzolillo and S. Sennato: conceptualization, methodology, investigation, data analysis, writing - original draft, writing - review and editing, supervision; L. Di Marzio: funding acquisition, writing - review; M.Carafa: funding acquisition, supervision, writing - review; C. Marianecci: writing - review; F. Bordi: conceptualization, writing - review, funding acquisition, supervision.

Declaration of Competing Interest

The authors declare that they have no known competing financial interests or personal relationships that could have appeared to influence the work reported in this paper.

Acknowledgments

This research was funded by Phospholipid Research Center (Grant n. FBO-2017-051/1-1). F.S and S. T. acknowledge support from Torno Subito projects of Lazio Adisu-Regione Lazio; S. S. thanks S. Casciardi for TEM microscopy and C. Bombelli and F. Ceccacci for use of Minitrough and for scientific discussions.

References

[1] World Health Organization, Global Tuberculosis Report 2019, Tech. rep. (2019).

[2] K. Xu, Z. C. Liang, X. Ding, H. Hu, S. Liu, M. Nurmik, S. Bi, F. Hu, Z. Ji, J. Ren, et al., Nanomaterials in the prevention, diagnosis, and treatment of Mycobacterium tuberculosis infections, Advanced healthcare materials 7 (2018) 1700509.

[3] P. Deol, G. Khuller, K. Joshi, Therapeutic efficacies of isoniazid and rifampin encapsulated in lung-specific stealth liposomes against mycobacterium tuberculosis infection induced in mice, Antimicrobial agents and chemotherapy 41 (1997) 1211–1214.

[4] D. C. Quenelle, J. K. Staas, G. A. Winchester, E. L. Barrow, W. W. Barrow, Efficacy of microencapsulated rifampin in mycobacterium tuberculosis-infected mice, Antimicrobial agents and chemotherapy 43 (1999) 1144–1151.

[5] C. Marianecci, L. Di Marzio, F. Rinaldi, M. Carafa, F. Alhaique, et al., Pulmonary delivery: innovative approaches and perspectives, Journal of Biomaterials and Nanobiotechnology 2 (2011) 567–575.

[6] P. Preziosi, Isoniazid: metabolic aspects and toxicological correlates, Current drug metabolism 8 (2007) 839–851.

[7] C. Rodrigues, P. Gameiro, S. Reis, J. Lima, B. de Castro, Spectrophotometric determination of drug partition coefficients in dimyristoyl-l-α-phosphatidylcholine/water: a comparative study using phase separation and liposome suspensions, Analytica chimica acta 428 (2001) 103–109.

[8] A. D. Bangham, M. M. Standish, J. C. Watkins, Diffusion of univalent ions across the lamellae of swollen phospholipids, Journal of molecular biology 13 (1965) 238–252.

[9] R. Abra, C. A. Hunt, D. Lau, Liposome disposition in vivo VI: delivery to the lung, Journal of pharmaceutical sciences 73 (1984) 203–206.

[10] R. Pandey, S. Sharma, G. Khuller, Liposome-based antitubercular drug therapy in a guinea pig model of tuberculosis, International journal of antimicrobial agents 23 (2004) 414–415.

[11] O. R. Justo, Â. M. Moraes, Incorporation of antibiotics in liposomes designed for tuberculosis therapy by inhalation, Drug delivery 10 (2003) 201–207.

[12] A. Gürsoy, E. Kut, S. Özkırımlı, Co-encapsulation of isoniazid and rifampicin in liposomes and characterization of liposomes by derivative spectroscopy, International journal of pharmaceutics 271 (2004) 115–123.

[13] G. Chimote, R. Banerjee, In vitro evaluation of inhalable isoniazid-loaded surfactant liposomes as an adjunct therapy in pulmonary tuberculosis, Journal of Biomedical Materials Research Part B: Applied Biomaterials 94 (2010) 1–10.

[14] C. I. Nkanga, R. W. Krause, X. S. Noundou, R. B. Walker, Preparation and characterization of isoniazid-loaded crude soybean lecithin liposomes, International journal of pharmaceutics 526 (2017) 466–473.
[15] N. Kosa, B. Bocskei-Antal, K. Horváti, S. Bosze, L. Herenyi, I. Voszka, Investigation of encapsulated liposomal antituberculotics and effects on in vitro model systems, Biophysical Journal 110 (2016) 246a–247a.
[16] E. Truzzi, F. Meneghetti, M. Mori, L. Costantino, V. Iannuccelli, E. Maretti, F. Domenici, C. Castellano, S. Rogers, A. Capocefalo, et al., Drugs/lamellae interface influences the inner structure of double-loaded liposomes for inhaled anti-TB therapy: an in-depth small-angle neutron scattering investigation, Journal of colloid and interface science 541 (2019) 399–406.
[17] S. Bremer-Hoffmann, B. Halamoda-Kenzaoui, S. E. Borgos, Identification of regulatory needs for nanomedicines, Journal of Interdisciplinary Nanomedicine 3 (2018) 4–15.
[18] M. Wasserman, R. M. Beltrán, F. O. Quintana, P. M. Mendoza, L. C. Orozco, G. Rodriguez, A simple technique for entrapping rifampicin and isoniazid into liposomes, Tubercle 67 (1986) 83–90.
[19] R. W. Niven, H. Schreier, Nebulization of liposomes. i. Effects of lipid composition, Pharmaceutical research 7 (1990) 1127–1133.
[20] Q. T. Zhou, S. S. Y. Leung, P. Tang, T. Parumasivam, Z. H. Loh, H.-K. Chan, Inhaled formulations and pulmonary drug delivery systems for respiratory infections, Advanced drug delivery reviews 85 (2015) 83–99.
[21] T. M. M Ways, W. M. Lau, V. V. Khutoryanskiy, Chitosan and its derivatives for application in mucoadhesive drug delivery systems, Polymers 10 (2018) 267.
[22] C. Rodrigues, P. Gameiro, M. Prieto, B. de Castro, Interaction of rifampicin and isoniazid with large unilamellar liposomes: spectroscopic location studies, Biochimica et Biophysica Acta (BBA) - General Subjects 1620 (2003) 151–159.
[23] G. Chimote, R. Banerjee, Evaluation of antitubercular drug insertion into preformed dipalmitoylphosphatidylcholine monolayers, Colloids and Surfaces B: Biointerfaces 62 (2008) 258–264.
[24] M. Pinheiro, A. S. Silva, S. Pisco, S. Reis, Interactions of isoniazid with membrane models: Implications for drug mechanism of action, Chemistry and physics of lipids 183 (2014) 184–190.
[25] C. Bombelli, G. Caracciolo, P. Di Profio, M. Diociaiuti, P. Luciani, G. Mancini, C. Mazzuca, M. Marra, A. Molinari, D. Monti, et al., Inclusion of a photosensitizer in liposomes formed by dmpc/gemini surfactant: correlation between physicochemical and biological features of the complexes, Journal of medicinal chemistry 48 (15) (2005) 4882–4891.
[26] D. E. Koppel, Analysis of macromolecular polydispersity in intensity correlation spectroscopy: the method of cumulants, The Journal of Chemical Physics 57 (1972) 4814–4820.
[27] S. Sennato, L. Carlini, D. Truzzolillo, F. Bordi, Salt-induced reentrant stability of polyion-decorated particles with tunable surface charge density, Colloids and Surfaces B: Biointerfaces 137 (2016) 109–120.
[28] F. Li, R. Schafer, C.-T. Hwang, C. E. Tanner, S. T. Ruggiero, High-precision sizing of nanoparticles by laser transmission spectroscopy, Applied optics 49 (2010) 6602–6611.
[29] A. De Marcellis, A. Sarra, G. D. P. Stanchieri, F. Bruni, F. Bordi, E. Palange, P. Postorino, Balanced laser transmission spectroscopy based on a tunable gain double channel LIA for nanoparticles detection in biomedical applications, in: 2019 IEEE Biomedical Circuits and Systems Conference (BioCAS), IEEE, 2019, pp. 1–4.
[30] M. De Robertis, A. Sarra, V. D'Oria, F. Mura, F. Bordi, P. Postorino, D. Fratantonio, Blueberry-derived exosome-like nanoparticles counter the response to TNF-α-induced change on gene expression in EA-hy926 cells, Biomolecules 10 (2020) 742.
[31] M. Shinitzky, Y. Barenholz, Fluidity parameters of lipid regions determined by fluorescence polarization, Biochimica et Biophysica Acta (BBA)-Reviews on Biomembranes 515 (1978) 367–394.
[32] N. Barsoum, M. S. Kamel, M. M. Diab, Spectrophotometric determination of isoniazid and rifampicin from pharmaceutical preparations and biological fluids, Research Journal of Agricultural and Biological Sciences 4 (2008) 471–484.
[33] B. J. Berne, R. Pecora, Dynamic Light scattering with application to chemistry, biology, and physics, Dover Publications, Inc, 2000.
[34] G. Roberts, Langmuir-Blodgett Films, Plenum Press, New York, 1990.
[35] F. Bordi, C. Cametti, S. Sennato, B. Paoli, C. Marianecci, Charge renormalization in planar and spherical charged lipidic aqueous interfaces, The Journal of Physical Chemistry B 110 (2006) 4808–4814.
[36] D. Marsh, Lateral pressure in membranes, Biochimica et Biophysica Acta (BBA) - Reviews on Biomembranes 1286 (1996) 183–223.
[37] S. Sennato, F. Bordi, C. Cametti, C. Coluzza, A. Desideri, S. Rufini, Evidence of domain formation in cardiolipin-glycerophospholipid mixed monolayers. A thermodynamic and AFM study, The Journal of Physical Chemistry B 109 (2005) 15950–15957.
[38] O. Szekely, A. Steiner, P. Szekely, E. Amit, R. Asor, C. Tamburu, U. Raviv, The structure of ions and zwitterionic lipids regulates the charge of dipolar membranes, Langmuir 27 (2011) 7419–7438.
[39] R. Zimmermann, D. Küttner, L. Renner, M. Kaufmann, J. Zitzmann, M. Müller, C. Werner, Charging and structure of zwitterionic supported bilayer lipid membranes studied by streaming current measurements, fluorescence microscopy, and attenuated total reflection fourier transform infrared spectroscopy, Biointerphases 4 (2009) 1–6.
[40] N. J. Zuidam, H. M. E. Gouw, Y. Barenholz, D. J. Crommelin, Physical (in)stability of liposomes upon chemical hydrolysis: the role of lysophospholipids and fatty acids, Biochimica et Biophysica Acta (BBA)-Biomembranes 1240 (1995) 101–110.
[41] Y. Okahata, H.-j. Lim, S. Hachiya, G.-i. Nakamura, Bilayer-coated capsule membranes. IV.: Control of NaCl permeability by phase transition of synthetic bilayer coatings, depending on their hydrophilic head groups, Journal of Membrane Science 19 (1984) 237–247.
[42] X. Xu, M. A. Khan, D. J. Burgess, Predicting hydrophilic drug encapsulation inside unilamellar liposomes, International journal of pharmaceutics 423 (2012) 410–418.
[43] H. Kitayama, Y. Takechi, N. Tamai, H. Matsuki, C. Yomota, H. Saito, Thermotropic phase behavior of hydrogenated soybean phosphatidylcholine–cholesterol binary liposome membrane, Chemical and Pharmaceutical Bulletin 62 (2014) 58–63.
[44] G. G. Putzel, M. Schick, Phase behavior of a model bilayer membrane with coupled leaves, Biophysical journal 94 (2008) 869–877.
[45] A. V. Marques, P. M. T. Júnior, S. Marques, T. Brum, E. Harte, M. O. Rodrigues, M. G. Montes D′Oca, P. A. da Silva, A. R. Pohlmann, I. D. Alves, et al., Isoniazid interaction with phosphatidylcholine-based membranes, Journal of Molecular Structure 1051 (2013) 237–243.
[46] G. Rajalakshmi, B. Devipriya, A. R. Parameswari, A. D. Stephen, P. Kumaradhas, Understanding the N-N bond cleavage and the electrostatic properties of isoniazid drug molecule via theoretical charge density study, Computational and Theoretical Chemistry 966 (2011) 259–264.
[47] A. k. Pandey, A. Bajpai, V. Baboo, A. Dwivedi, Structural, electronic, and vibrational properties of isoniazid and its derivative n-cyclopentylidenepyridine-4-carbohydrazide: a quantum chemical study, Journal of Theoretical Chemistry 2014 (2014).
[48] S. A. Kane, S. D. Floyd, Interaction of local anesthetics with phospholipids in langmuir monolayers, Physical Review E 62 (2000) 8400.
[49] A. Kõiv, P. Mustonen, P. K. Kinnunen, Differential scanning calorimetry study on the binding of nucleic acids to dimyristoylphosphatidylcholine-sphingosine liposomes, Chemistry and physics of lipids 70 (1994) 1–10.
[50] P. A. Forsyth Jr, S. Marčelja, D. J. Mitchell, B. W. Ninham, Phase transition in charged lipid membranes, Biochimica et Biophysica Acta (BBA)-Biomembranes 469 (1977) 335–344.
[51] S. Giatrellis, G. Nounesis, Nucleic acid-lipid membrane interactions studied by dsc, Journal of Pharmacy and Bioallied Sciences 3 (2011) 70.
[52] A. Iglič, P. A. Beales, Advances in Planar Lipid Bilayers and Liposomes, Vol. 20, Elsevier, 2014.
[53] D. Harries, S. May, W. M. Gelbart, A. Ben-Shaul, Structure, stability, and thermodynamics of lamellar DNA-lipid complexes, Biophysical journal 75 (1998) 159–173.
[54] R. Bruinsma, J. Mashl, Long-range electrostatic interaction in DNA-cationic lipid complexes, EPL (Europhysics Letters) 41 (1998) 165.
[55] J. Sabın, G. Prieto, J. M. Ruso, R. Hidalgo-Alvarez, F. Sarmiento, Size and stability of liposomes: a possible role of hydration and osmotic forces, The European Physical Journal E 20 (2006) 401–408.
[56] M. A. Wilson, A. Pohorille, Adsorption and Solvation of Ethanol at the Water LiquidâĹŠVapor Interface: A Molecular Dynamics Study, The Journal of Physical Chemistry B 101 (1997) 3130–3135.
[57] G. S. Longo, M. Schick, I. Szleifer, Stability and liquid-liquid phase separation in mixed saturated lipid bilayers, Biophysical journal 96 (2009) 3977–3986.
[58] F. A. Heberle, G. W. Feigenson, Phase separation in lipid membranes,

Cold Spring Harbor perspectives in biology 3 (2011) a004630.
[59] N. Saikia, R. C. Deka, Density functional study on the adsorption of the drug isoniazid onto pristine and B-doped single wall carbon nanotubes, Journal of molecular modeling 19 (2013) 215–226.
[60] M. Pinheiro, J. Magalhães, S. Reis, Antibiotic interactions using liposomes as model lipid membranes, Chemistry and physics of lipids 222 (2019) 36–46.
[61] I. M. Le-Deygen, A. A. Skuredina, A. S. Safronova, I. D. Yakimov, I. M. Kolmogorov, D. M. Deygen, T. V. Burova, N. V. Grinberg, V. Y. Grinberg, E. V. Kudryashova, Moxifloxacin interacts with lipid bilayer, causing dramatic changes in its structure and phase transitions, Chemistry and Physics of Lipids 228 (2020) 104891.